

## THE EFFECT OF $Mn^{+2}$ DOPING RATIO ON THE SENSING PROPERTIES OF $CoFe_2O_4$ NANOPARTICLES FOR $CO_2$ AND $NH_3$ GASES

Rihab JABBAR<sup>1\*</sup>, Sabah H. SABEEH<sup>2</sup>, Awham M. HAMEED<sup>3</sup>

*In this work, undoped and manganese ( $Mn^{+2}$ ) doped spinel cobalt ferrites nanoparticles (NPs) having a composition ( $Mn_xCo_{1-x}Fe_2O_4$  where  $x = 0.2$  and  $0.8$ ) were synthesis by sol-gel precipitation method. The results showed that the average crystallite size ( $D$ ) was found to decrease from  $20.68$  nm to  $9.95$  nm with increasing the  $Mn^{+2}$  doping ratio. The samples have flat surface morphology as indicated by SEM and the grain sizes decrease with increasing the Mn-doping ratio as indicated by AFM. The sensing property was carried out at room temperature for  $CO_2$  and  $NH_3$  gases. It observed that all sample with different compositions sensitive to both gases, where the  $Mn_{0.8}Co_{0.2}Fe_2O_4$  samples have the highest sensitivity for  $CO_2$  and  $NH_3$  were  $32.12\%$  and  $98\%$  respectively.*

**Keywords:**  $CoFe_2O_4$ , Nanoparticles, Gas Sensor, Sol-Gel method. Mn-doped  $CoFe_2O_4$ ,  $CO_2$ ,  $NH_3$

### 1. Introduction

Nowadays, the great effect of poisonous gases like  $CO$ ,  $CO_2$ ,  $NO$ , and  $NO_2$  on the environmental damage resulting from automobile exhausts has become progressively clear as well as  $Cl_2$ ,  $CH_4$ , and  $NH_3$  gases resulting from the industrial operations [1]. Therefore, the metal oxide gas sensor, especially the spinel ferrites in the general formula ( $MB_2O_4$ ) ( $M$  = bivalent metal ions, such as  $Mn$ ,  $Fe$ ,  $Mg$ ,  $Zn$ ,  $Ni$ ,  $Co$ ,  $Cu$ , etc.) in which the metal cations  $M$  and  $B$  are positioned at A-site (tetrahedral) and B-sites (octahedral) sublattice and oxygen has an (FCC) close packing structure, it had attracted more interest in recent years due to their properties such as low cost, good chemical properties, good thermal properties, rapid response and recovery time and modest electronic design. Moreover, it can be provided substantial sensitivity, selectivity, and stability required by these systems [2, 3]. Among these spinel ferrites, cobalt ferrite ( $CoFe_2O_4$ ) essentially interesting due to its properties that includes chemical stability, mechanical hardness, strong anisotropy, high forced field and moderate saturation magnetization [4].

<sup>1,2,3</sup> Department of Applied Sciences, University of Technology, Baghdad, Iraq,

\* Corresponding author's e-mail: rihabjabbar@yahoo.com

The structural, magnetic and electrical properties of  $(\text{CoFe}_2\text{O}_4)$  can be changed by metal dopants ions such as  $\text{Mn}^{+2}$ ,  $\text{Mg}^{+2}$ ,  $\text{Zn}^{+2}$ ,  $\text{Ni}^{+2}$ , etc. The new system has desired properties and therefore it has found increasing attention in the sensor, high-frequency applications and activators [5, 6]. The metal gas sensor is the most commonly used sensors at room temperature and even at elevated temperatures because of its advantages that mentioned above, except for the small types of polymer gas matrix sensors which work at high temperature [7, 8]. Many studies have been carried out in the literature to explore the sensing properties of the metal oxides especially the spinel ferrite for different types of gases.

Sun et al. [9] they had stated the sensing properties of  $\text{CuFe}_2\text{O}_4$  nanoparticles for some gases like ethanol, hydrogen, ammonia, and acetone. Their results showed a high response to ethanol. On the other hand, Kamble and Mathe [10] they had studied the nanocrystalline synthesis of  $\text{NiFe}_2\text{O}_4$  as a metal gas sensor using different gases such as  $\text{O}_2$ , liquid petroleum gas (LPG),  $\text{NH}_3$  and  $\text{Cl}_2$ . They found that the nickel ferrite nanoparticles are more sensitive to  $\text{Cl}_2$  and  $\text{NH}_3$  than other gases.

Christine et al. [11] they had pointed out the sensing properties of nanoparticles cobalt ferrite with a different composition for  $\text{NH}_3$  gas. Their results showed that the cobalt ferrite has a very high response, good sensitivity and good reversibility as a metal gas sensor. Kumar et al. [12] also they had studied the substituted of  $\text{Mn}^{+2}$  by copper ferrite nanoparticles synthesis as a metal gas sensor and the effect of some gases such as LPG,  $\text{H}_2$ ,  $\text{NH}_3$ ,  $\text{CO}$ , ethanol, and methanol; their results show that  $\text{Mn}^{+2}$  which substituted with copper ferrite nanoparticles has high sensitivity to LPG. Moreover, Devi et al. [13] they had reported the sensing properties of Mn-Doped  $\text{CoFe}_2\text{O}_4$  nanoparticles for ethanol gas, they found improvement in ethanol gas sensitivity with an increase in  $\text{Mn}^{+2}$  doping ratio.

This work aims to study the role of Mn-doping ratio on the sensing properties of cobalt ferrite nanoparticles for the possibility of synthesizing a good metallic gas sensor working at room temperature and also to determine the sensitivity of  $\text{CO}_2$  and  $\text{NH}_3$  gases at room temperature.

## 2. Experimental details

### 2.1. Synthesis of undoped and Mn-doping of $\text{CoFe}_2\text{O}_4$

It has been examining the nanoparticles of undoped  $\text{CoFe}_2\text{O}_4$  cobalt ferrite and  $\text{CoFe}_2\text{O}_4$  cobalt ferrite doped with manganese (Mn) according to formula  $(\text{Mn}_x\text{Co}_{1-x}\text{Fe}_2\text{O}_4)$  were  $x = 0.2$  and  $0.8$  which synthesized by the sol-gel precipitation method. A stoichiometric ratio of cobalt chloride ( $\text{CoCl}_2 \cdot 6\text{H}_2\text{O}$ ), manganese chloride ( $\text{MnCl}_2 \cdot 4\text{H}_2\text{O}$ ) and ferric chloride ( $\text{FeCl}_3$ ) BDH with a purity above 97 % were dissolved in distilled water using a magnetic stirrer. Then, 2 M

of NaOH solution was added to the mixture slowly like a drop with continuous stirring for 90 min where the pH value of solution adjusted to 13, after that the mixture was heated to (100 ± 5 °C) for two hours with continuous stirring, the solution converts gradually to wet gel with black color then the wet gel converted completely to powder by leave it on hot plate at 200 °C. The produced powder was washed five times with distilled water and ethanol to remove NaCl and any other impurities.

## 2.2 Characterization Studies

The structural properties of prepared cobalt ferrite were investigated by X-ray diffraction using Philips PW 1050 X-ray diffractometer of  $\lambda = 1.5 \text{ \AA}^\circ$  from Cu- $\text{K}\alpha$  and Fourier-Transform Infrared Spectroscopy (FTIR) in rang (400-4000  $\text{cm}^{-1}$ ) (SHIMADZU). The surface morphology was investigated by Scanning Electron Microscopy (SEM); model (INSPECT S50 (FEI)-Netherlands) and Atomic Force Microscopy (AFM); model (CSPM-AA3000 Japan).

## 2.3 Gas sensor process

The sensing properties of CO<sub>2</sub> and NH<sub>3</sub> gases were carried out on prepared powders pellets with different compositions. The pellets are synthesis using a die with (1 cm) in diameter, where (1 gram) of powder was pressed by a hydraulic piston with force equal to 1 ton for 2 minutes. Then the synthesis pellets are sintering at 1000 °C for two hours within the furnace; model Nabertherm GmbH – Germany. The silver electrodes were deposited on the sintered pellets as shown in figure 1 to measure the change in the electrical resistance. The sensor sensitivity (S) is defined as [14]:

$$S = \frac{R_0 - R_{gs}}{R_{gs}} \approx \frac{R_0}{R_{gs}} \quad \text{if} \quad R_{gs} \ll R_0 \quad (1)$$

or

$$S = \frac{R_{gs} - R_0}{R_0} \approx \frac{R_{gs}}{R_0} \quad \text{if} \quad R_{gs} \gg R_0$$

where,

R<sub>o</sub> - the sensor resistance in air;

R<sub>gs</sub> - the sensor resistance in the presence of gas.

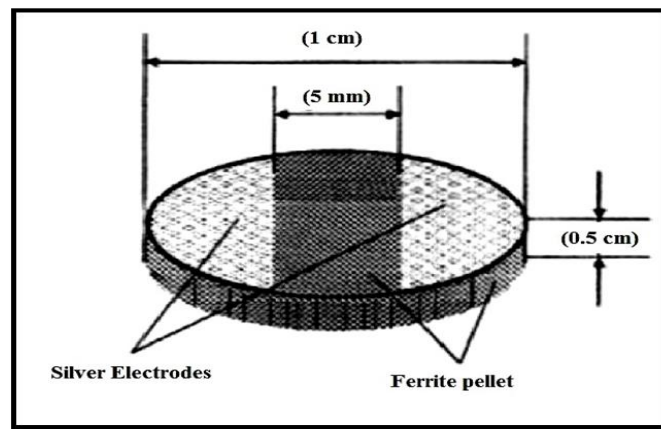


Fig. 1. Design of ferrite pellet with silver electrodes for gas sensor.

### 3. Results and Discussion

#### 3.1 X-ray diffraction results

Figure 2 shown the X-Ray Diffraction (XRD) patterns of  $\text{CoFe}_2\text{O}_4$ ,  $\text{Mn}_{0.2}\text{Co}_{0.8}\text{Fe}_2\text{O}_4$  and  $\text{Mn}_{0.8}\text{Co}_{0.2}\text{Fe}_2\text{O}_4$  nanoparticles, the observed peaks which are (220), (311), (222), (400), (422), (511) and (440) compared to the standard data (JCPDS PDF card No. 22-1086) revealing to the cubic spinel structure of the cobalt ferrite.

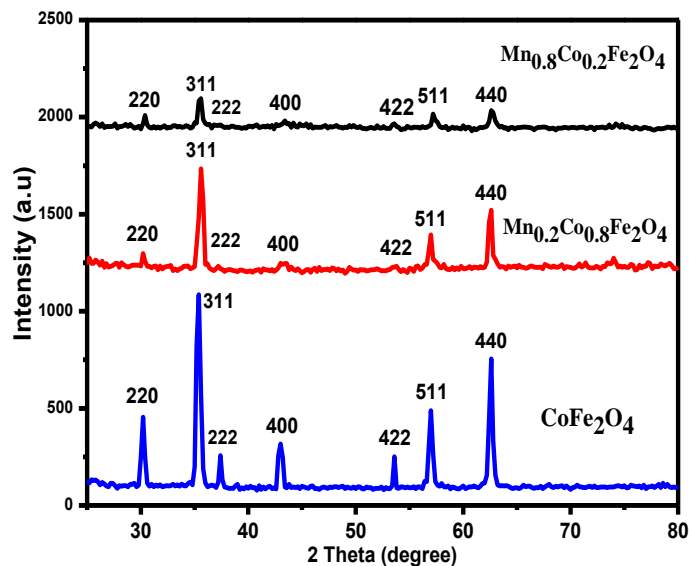


Fig. 2. XRD pattern of the undoped and Mn-doped of  $\text{CoFe}_2\text{O}_4$

The diffraction peaks did not appear because of Mn doping, therefore it does not influence on the cubic structure of CoFe<sub>2</sub>O<sub>4</sub>. The average of crystallite size (D) was calculated using the Scherrer-Debye equation from the highest peak which is (311) [15]:

$$D = \frac{0.9\lambda}{\beta \cos \theta} \quad (3)$$

It has been found that the crystal size average of CoFe<sub>2</sub>O<sub>4</sub> decreased to 16.89 nm, while Mn<sub>0.8</sub>Co<sub>0.2</sub>Fe<sub>2</sub>O<sub>4</sub> to 12.85 nm, these decreases in the crystallite size with an increase in Mn<sup>+2</sup> doping ratio were observed by Shobana et al. [16] and P. Indra Devi et al. [13]. The X-ray density (d) was calculated by the following relation [17]:

$$d = \frac{8M}{Na^3} \quad (4)$$

where,

M - the molecular weight of the cobalt ferrite;

N - Avogadro number;

a - the lattice constant.

The apparent porosity of the samples was calculated from the following relation [18]:

$$(P\%) = \frac{Ws - Wd}{Ws - Wi} \times 100 \% \quad (5)$$

where,

Ws - the wet specimen weight;

Wd - the dry weight of the specimen;

Wi - the emerge weight of the specimen.

The ionic radius of Co<sup>+2</sup> ions is (0.71 °A) and the ionic radius of Mn<sup>+2</sup> is (0.67 °A), this decrease in the lattice constant (a) with increase the Mn<sup>+2</sup> doping ratio as listed in Table 1 due to the large Co<sup>+2</sup> ions replaced by the small Mn<sup>+2</sup> ions.

Table 1

XRD parameters of Undoped and Mn-doped CoFe<sub>2</sub>O<sub>4</sub>

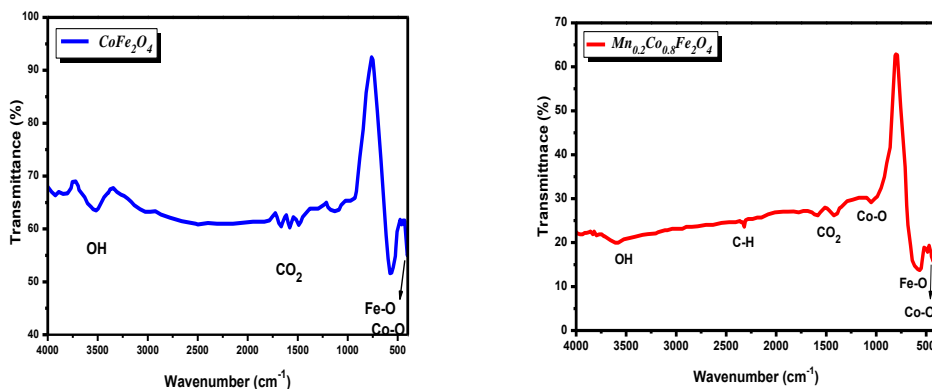
Samples	hkl	D (nm)	D ave. (nm)	a (A)	d (A)	d	P (%)
CoFe <sub>2</sub> O <sub>4</sub>	311	20.68	16.89	8.3753	2.5252	5.45	27
	400	14.58		8.2540	1.5885		
	511	15.41		8.2703	1.4620		

$Mn_{0.2}Co_{0.8}Fe_2O_4$	311	10.79	12.54	8.3533	2.5186	5.29	5
	400	11.22		8.3943	1.6154		
	511	15.63		8.4000	1.4849		
$Mn_{0.8}Co_{0.2}Fe_2O_4$	311	9.95	12.85	8.3596	2.5205	5.32	13
	400	14.57		8.3495	1.6068		
	511	14.03		8.3779	1.4810		

Also, it can be noticed in figure 2 that the intensities of the peaks decrease with increase the doping ratio in the samples and this may be due to decreasing the crystals of  $CoFe_2O_4$  with increase the  $Mn^{+2}$  content.

### 3.2 FTIR analysis

Figure 3 shows FTIR spectra of cobalt ferrite nanoparticles and  $CoFe_2O_4$  doping with  $Mn^{+2}$ . The bands that were observed in the ranges of  $408.92 - 459.07\text{ cm}^{-1}$  and  $513.94 - 588.31\text{ cm}^{-1}$  are for the octahedral group (Co-O) and the tetrahedral group (Fe-O) respectively which indicate the formation of the spinel structure. The observed bands of undoped  $CoFe_2O_4$  was  $1078.24\text{ cm}^{-1}$ , while for doped  $CoFe_2O_4$  with Mn at 0.2 and 0.8 were  $1033.88\text{ cm}^{-1}$  and  $1026.16\text{ cm}^{-1}$  respectively which designate the formation of Co-substituted spinel ferrites [19]. The  $CO_2$  absorption was observed at range ( $1448.59 - 1649.19\text{ cm}^{-1}$ ). The peak value is about ( $2362.88\text{ cm}^{-1}$ ) in  $CoFe_2O_4$  sample and is about ( $2360.95\text{ cm}^{-1}$ ) for  $CoFe_2O_4$  doping with  $Mn^{+2}$  on the aliphatic and aromatic C-H stretching bond. C-H stretching bundle was observed in  $CoFe_2O_4$  sample at about ( $3030.27\text{ cm}^{-1}$ ) the above-observed bands confirm the presence of organic impurities in samples during synthesis conditions. Other bundles were observed at range ( $3423.76 - 3742.03\text{ cm}^{-1}$ ) related to the stretching vibration of the hydroxyl group.



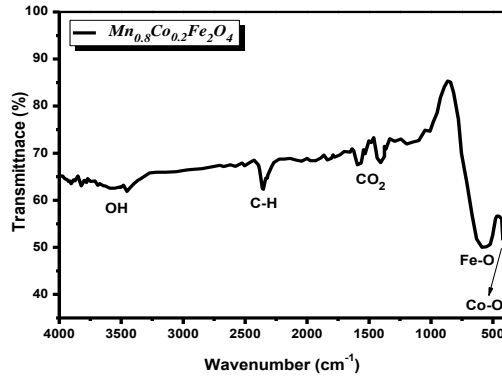
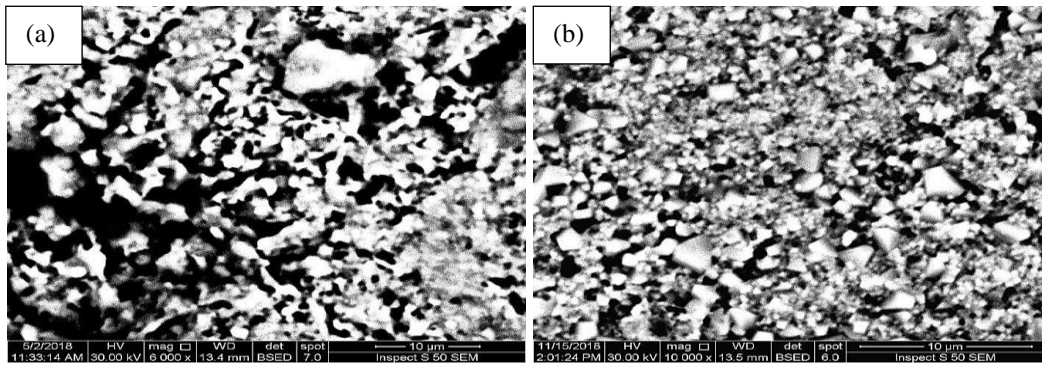


Fig. 3. FTIR pattern of the undoped and Mn-doped  $CoFe_2O_4$

### 3.3 Morphological study

Figure 4 a, b and c shows SEM images of prepared samples. The images show a good homogeneous distribution of flat nanoparticles of prepared samples with a different composition. Figure 5 shows 3-Dimensional images by AFM of prepared samples with different compositions. As shown in figures 4, 5 and Table 2, it can see that the doping manganese ions  $Mn^{+2}$  did not effect on the shape and the surface morphology of the  $CoFe_2O_4$ , where it remains as the columnar structure but the grain size decrease with increase the doping ratio.



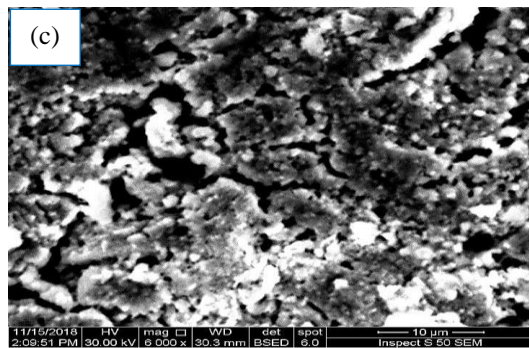


Fig. 4. SEM image of (a)  $\text{CoFe}_2\text{O}_4$ , (b)  $\text{Mn}_{0.2}\text{Co}_{0.8}\text{Fe}_2\text{O}_4$ , (c)  $\text{Mn}_{0.8}\text{Co}_{0.2}\text{Fe}_2\text{O}_4$ .

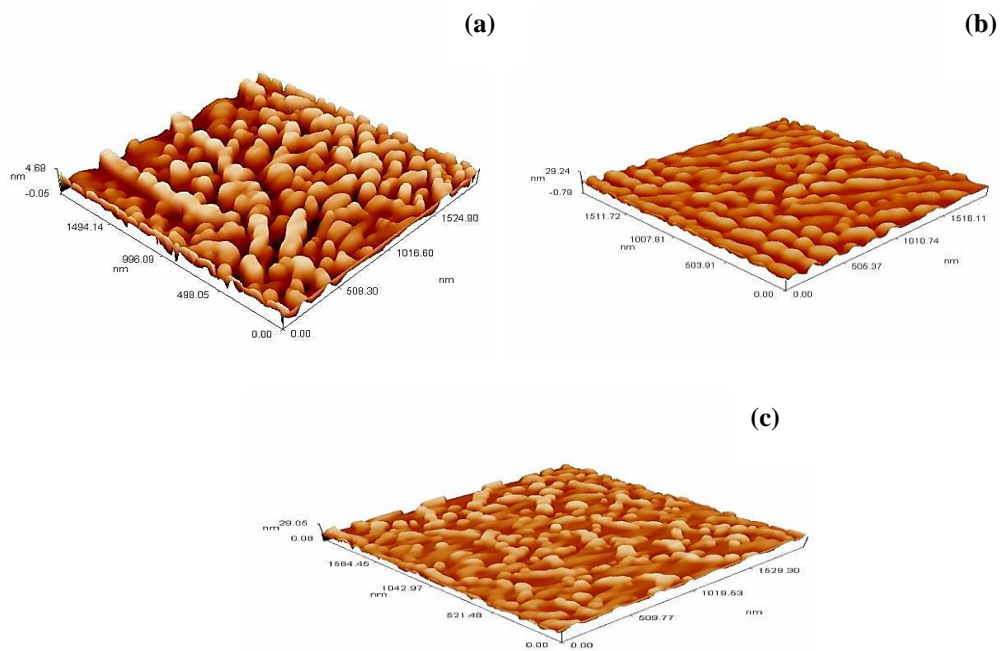


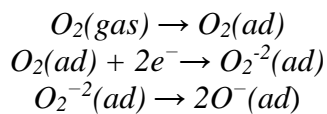
Fig. 5. 3D-Images by AFM for (a)  $\text{CoFe}_2\text{O}_4$ , (b)  $\text{Mn}_{0.2}\text{Co}_{0.8}\text{Fe}_2\text{O}_4$ , (c)  $\text{Mn}_{0.8}\text{Co}_{0.2}\text{Fe}_2\text{O}_4$ .

*Table 2*  
**Average grain size, surface roughness, and Root mean square of Undoped and Mn-doped  $\text{CoFe}_2\text{O}_4$**

Samples	Grain size (nm)	Roughness (nm)	Root mean square(nm)
$\text{CoFe}_2\text{O}_4$	120	0.93	1.08
$\text{Mn}_{0.2}\text{Co}_{0.8}\text{Fe}_2\text{O}_4$	87.90	2.85	3.27
$\text{Mn}_{0.8}\text{Co}_{0.2}\text{Fe}_2\text{O}_4$	79.55	2.68	3.15

### 3.4 Sensing properties

In fact, the gas sensing mechanism depending on that metal oxide sample composed of a great number of small grains connected at their boundaries, therefore the lower the grain size, the greater the sensitivity of samples toward gases [20]. The behavior of the gas sensor depends on the sensor located below the different gases on various factors such as the reaction between the gas absorption and absorbed oxygen, the variation in the absorption process and the quantity of absorbed oxygen. The adsorption and ionization of oxygen in the existence of the gas being sensed can be estimated in the following equations:



The entering gas allows in desorption of the oxygen by release the electron and therefore changes the carrier behavior of the sensor [21, 22]. The principle of chemco-resistance is responsible for varying the electrical resistance of any metal oxide gas sensor on exposure to a home gas [23]. Adsorbed gas molecules react with the metal oxide which acts as an emitter or receiver of charge carriers and varying the resistance of the metal oxide. Type of the gas which can be either oxidizing or reducing and the type of the major carriers existing in the metal oxide influence on the resistance of the metal oxide. Moreover, the surface morphology and the grain size of the metal oxide play an important role in the sensing properties in the gas sensor devices. The response time is determining at the time desired for the difference in behavior reach 90% of the equalizer value then after that the test gas is injected. The recovery time is the time need for the sensor to return to its main behavior in the air [12].

The gas sensing properties of the CoFe<sub>2</sub>O<sub>4</sub>, Mn<sub>0.2</sub>Co<sub>0.8</sub>Fe<sub>2</sub>O<sub>4</sub> and Mn<sub>0.8</sub>Co<sub>0.2</sub>Fe<sub>2</sub>O<sub>4</sub> nanoparticles have been established for both CO<sub>2</sub> and NH<sub>3</sub> gases. The response of gases at the surface of the nanoparticles was estimated in the form of sensitivity % using equation (1) at 200 ppm. Firstly the gas sensor (pellet) resistance measured in the air in the dome chamber then gases was inserted in the chamber. Once the insertion of these gases; the samples pellet exhibited an increase in the sensor response. The response increased up to 50% through 3 minutes and it reached a steady state at about 7 minutes.

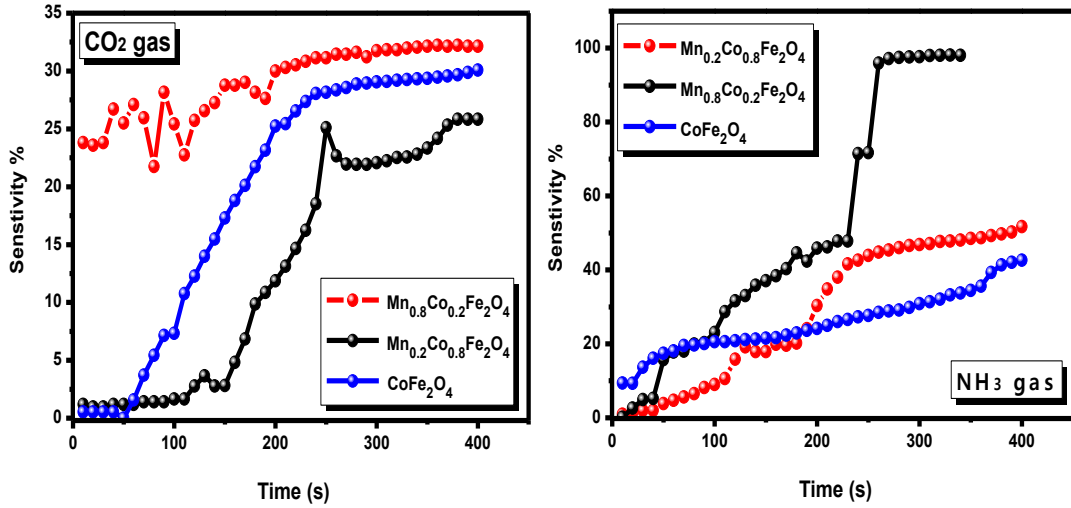


Fig. 6. Gas sensitivity of  $\text{CoFe}_2\text{O}_4$ ,  $\text{Mn}_{0.2}\text{Co}_{0.8}\text{Fe}_2\text{O}_4$  and  $\text{Mn}_{0.8}\text{Co}_{0.2}\text{Fe}_2\text{O}_4$  respectively, for both  $\text{CO}_2$  and  $\text{NH}_3$  gases as a function of time.

It can be clearly seen that the gas sensitivity increased with increase Mn-doping ratio and this corresponds to  $\text{NH}_3$  gas, while in  $\text{CO}_2$  gas the  $\text{CoFe}_2\text{O}_4$  has higher sensitivity than  $\text{Mn}_{0.2}\text{Co}_{0.8}\text{Fe}_2\text{O}_4$  and the sensitivity of  $\text{Mn}_{0.8}\text{Co}_{0.2}\text{Fe}_2\text{O}_4$  for  $\text{CO}_2$  gas reaches to 32.13 which is a high value for this type of gas. The gas sensitivity of  $\text{Mn}_{0.8}\text{Co}_{0.2}\text{Fe}_2\text{O}_4$  sample for  $\text{NH}_3$  gas reaches 98 % and it is an excellent value. The increase in the sensitivity of gas is due to the reduction in the grain size by the increase of Mn-doping ratio. Where the small grain size provides higher surface area and the higher surface area meaning more reaction with the gases consequently increases the sensitivity of the sample, these obtained results are confirming the obtained results by D. Rathore et al. [22]. All samples have relative good response times which were (20 s) while they take around one hour to return the main resistance after elimination of gases from the locked chamber. The high recovery time of the samples was because of the large ease of the sensing element. When the pellets samples are exposing to  $\text{CO}_2$  and  $\text{NH}_3$  gases, they go deeper into the pellet and it takes place very slowly results in longer recovery time.

#### 4. Conclusion

The present paper aims mainly to examine the effect of Mn-doping on the sensing properties of cobalt ferrite nanoparticles to synthesizing a good metallic gas sensor working at room temperature. Undoped and Mn-doped  $\text{CoFe}_2\text{O}_4$  nanoparticles were successfully syntheses by sol-gel method. The gas sensor

properties of different CoFe<sub>2</sub>O<sub>4</sub> composition was investigated in term of sensitivity for two types of gases CO<sub>2</sub> and NH<sub>3</sub>. The sensing test shows that the prepared samples of CoFe<sub>2</sub>O<sub>4</sub>, Mn<sub>0.2</sub>Co<sub>0.8</sub>Fe<sub>2</sub>O<sub>4</sub> and Mn<sub>0.8</sub>Co<sub>0.2</sub>Fe<sub>2</sub>O<sub>4</sub> are sensitive for both gases use in the present experiment and the gas sensitivity increase with increasing the Mn<sup>+2</sup> doping ratio from 0.2 to 0.8. It can be concluded that doping of CoFe<sub>2</sub>O<sub>4</sub> with a metal ion can be improved the sensing properties, and Mn<sub>0.8</sub>Co<sub>0.2</sub>Fe<sub>2</sub>O<sub>4</sub> has an excellent gas sensor for NH<sub>3</sub> gas as well.

## REFERENCE

- [1]. *G. Eranna, B. C. Josha, D. P. Runthalaa, and R. P. Gupta*, “Oxide materials for the development of integrated gas sensors - A comprehensive review”, Crit Rev Solid State Mater Sci, **Vol. 29**, 2014, pp.111-188
- [2]. *Sh. Sun, H. Zeng, D. B. Robinson, S. Raoux, P.M. Rice, Sh. X. Wang and G. Li*, “Monodisperse MFe<sub>2</sub>O<sub>4</sub> (M ) Fe, Co, Mn) Nanoparticles”, J. Appl. Chem. Soc, **Vol. 126**, 2004, pp. 273-279
- [3]. *M. Sugimoto*, “The Past, Present, and Future of Ferrite”, J. Am. Ceram. Soc., **Vol. 82**, 1999, pp. 269–280.
- [4]. *B. Toksha, S. Shirsath, S. Patange, and K. Jadhav*, “Structural investigations and magnetic properties of cobalt ferrite nanoparticles prepared by sol-gel auto combustion method”, Sol. St. Com, **Vol. 147**, 2008, pp. 479–483
- [5]. *M. Ahsan, and F. Khan*, “Study of Structural, Electrical and Magnetic Properties of Manganese-Doped Cobalt Ferrite Nanoparticles with Non-stoichiometric Composition”, J. of Phy. Sci. and App. **Vol. 7**, 2017, pp. 30-37
- [6]. *A. Ayyappan, S. Mahadevan, P. Chandramohan, M. Srinivasan, J. Philip, and B. Raj*, “Influence of Co ion concentration on the size, magnetic properties, and purity of CoFe<sub>2</sub>O<sub>4</sub> spinel ferrite nanoparticles”, J. Phy. Chem. C, **Vol. 114**, 2010, pp. 6334–6341.
- [7]. *M. Madou, and S. Morrison*, “Chemical Sensing with Solid State Devices”, Academic Press, New York, 1989.
- [8]. *T. Janhavi, and D. Patil*, “Ammonia Gas Sensing Performance of Polyaniline-SnO<sub>2</sub>”, Inter. J. of Eng. Res. & Tech. **Vol. 5**, 2016, pp. 296-303
- [9]. *Z. Sun, L. Liu, D. Jia, and W. Pan*, “Simple synthesis of CuFe<sub>2</sub>O<sub>4</sub> nanoparticles as gas-sensing materials”, Sens. Actuators B., **Vol. 125**, 2007, pp.144–148
- [10]. *R. Kamble, V. Mathe*, “Nanocrystalline nickel ferrite thick film as an efficient gas sensor at room temperature”, Sensors and Actuators B, **Vol. 131**, 2008, pp.205–209
- [11]. *L. Christine, B. Marc, M. Véronique, A. Lilia, and M. Najeh*, “Nanoparticles of Cobalt Ferrite for NH<sub>3</sub> Sensing”, Sen. & Trans, **Vol. 27**, 2014, pp. 239-243
- [12]. *K. Ranjith, R. Jayaprakash, D. Indra, and P. SivaPrasadaReddy*, “Magnetic, dielectric and sensing properties of manganese substituted copper ferrite nanoparticles”, Journal of Mag. And Mag. Mate. **vol. 355**, 2014, pp.87–92
- [13]. *D. Indra, N. Rajkumar, B. Renganathan, D. Sastikumar, and K. Ramachandran*, “Ethanol Gas Sensing of Mn-Doped CoFe<sub>2</sub>O<sub>4</sub> Nanoparticles”, IEEE Sesns. J., **Vol. 11**, 2011, pp.1395-1402.
- [14]. *O. Varghese and C. Grimes* “Metal Oxide Nanostructures as Gas Sensors, In Encyclopedia of Nanoscience and Nanotechnology”, Ed. H.S. Nalwa, **Vol. 5**, 2004, pp.505-521
- [15]. *B. Cullity* “Element of X-ray Diffraction”, MA Google Scholar: Addison-Wesley Reading, 1978.

- [16]. *M. Shobana and M. Sankar*, “Characterization of sol-gel-prepared nano ferrites”, *J. Magn. Magn. Mater.*, **Vol. 321**, 2009, pp. 599–601
- [17]. *A. B. Shinde*, “Structural and electrical properties of cobalt ferrite nanoparticles”, *Inter. J. of Inn. Tech. and Exp. Eng.*, **Vol. 3**, 2013, pp.64-67
- [18] *S. Shigeyuki*, “Advanced technical ceramics”, 1st ed., Tokyo institute of technology, Japan, 1989, pp.151-226
- [19]. *M. Shyam, K. Ajit, and S. Shriram*, “Study on Synthesis and Characterization of  $\text{CoFe}_2\text{O}_4$  Nanoparticles”, *Inter. Con. on Bio, Environ. and Chem.*, **Vol. 46**, 2012, pp.92-95
- [20]. *B. Timmer, W. Olthuis, and A. Berg*, A. “Ammonia sensors and their applications - a review”, *Sens. Actuators B*, **Vol. 107**, 2005, pp. 666–677.
- [21]. *D. Rathore, R. Kurchania, and R. Pandey*, “Fabrication of  $\text{Ni}_{1-x}\text{Zn}_x\text{Fe}_2\text{O}_4$  ( $x = 0, 0.5$  and  $1$ ) nanoparticles gas sensor for some reducing gases”, *Sens. Actuators A*, **Vol. 199**, 2013, pp. 236–240.
- [22]. *D. Rathore, R. Kurchania, and R. Pandey*, “Gas sensing properties of size varying  $\text{CoFe}_2\text{O}_4$  nanoparticles”, *IEEE Sens.*, **Vol. 15**, 2015, pp.4961–4966.
- [23]. *P. Shankar, and J. Rayappan*, “Gas sensing mechanism of metal oxides: the role of the ambient atmosphere, type of semiconductor and gases-a review”, *Sci. Jet*, **Vol. 4**, 2015, pp.126-144.